**Atmospheric
Chemistry
and Physics
Discussions**

Water uptake of biomass burning aerosol at sub- and supersaturated conditions: closure studies and implications for the role of organics

U. Dusek[1,*], G. P. Frank[1,******], A. Massling[2,***], K. Zeromskiene[2,*****], Y. Iinuma[2], O. Schmid[1,**], G. Helas[1], T. Hennig[2,****], A. Wiedensohler[2], and M. O. Andreae[1]

[1]Max Planck Institute for Chemistry, Biogeochemistry Department, Mainz, Germany
[2]Leibnitz-Institute for Tropospheric Research, Leipzig, Germany
[*]now at: Institute for Marine and Atmospheric Sciences Utrecht, Utrecht University, Utrecht, The Netherlands
[**]now at: Comprehensive Pneumology Center, Institute of Lung Biology and Disease, Helmholtz Zentrum München, Germany
[***]now at: National Environmental Research Institute, Aarhus University, Roskilde, Denmark

---

ACPD

10, 29853–29895, 2010

Water uptake of biomass burning aerosol

U. Dusek et al.

Title Page

Abstract	Introduction
Conclusions	References
Tables	Figures

|◀ | ▶|
◀ | ▶

Back | Close

Full Screen / Esc

Printer-friendly Version

Interactive Discussion

**** now at: Department for Applied Environmental Science (ITM), Stockholm University, Stockholm, Sweden
***** now at: Dillon Consulting Ltd., Toronto, Canada
****** now at: Department of Physics, Lund University, Lund, Sweden

Correspondence to: U. Dusek (u.dusek@uu.nl)

Water uptake of biomass burning aerosol

U. Dusek et al.

Title Page

Abstract	Introduction
Conclusions	References
Tables	Figures

|◄ | ►|

◄ | ►

Back | Close

Full Screen / Esc

Printer-friendly Version

Interactive Discussion

Abstract

We investigate the CCN activity of freshly emitted biomass burning particles and their hygroscopic growth at a relative humidity (RH) of 85%. The particles were produced in the Mainz combustion laboratory by controlled burning of various wood types, peat and grass. The water uptake at sub- and supersaturations is parameterized by deriving a soluble volume fraction (ε). It is defined as the volume fraction of ammonium sulfate in the total aerosol material, which would be sufficient to explain the observed water uptake. For the wood burns, soluble volume fractions are low, generally around 0.11. This translates to a hygroscopicity parameter κ (another widely used parameterization; cf. Petters and Kreidenweis, 2007) of around 0.07. The main emphasis of this study is a comparison of ε derived from measurements at sub- and supersaturated conditions (ε_G and ε_CCN), in order to see whether the water uptake at 85% RH can predict the CCN properties of the biomass burning particles. Differences in ε_G and ε_CCN can arise through solution non-idealities, the presence of slightly soluble or surface active compounds, or non-spherical particle shape. We find that ε_G and ε_CCN agree within experimental uncertainties (of around 30%) for particle sizes of 100 and 150 nm; only for 50 nm particles is ε_CCN larger than ε_G by a factor of 2. The magnitude of this difference and its dependence on particle size is consistent with the presence of surface active organic compounds. These compounds mainly facilitate the CCN activation of small particles, which form the most concentrated solution droplets at the point of activation. The 50 nm particles, however, are only activated at supersaturations higher than 1% and are therefore of minor importance as CCN in ambient clouds. By comparison with the actual chemical composition of the biomass burning particles, we estimate that the hygroscopicity of the organic fraction is roughly 1/3 that of ammonium sulfate and can be represented by $\kappa = 0.15$–0.2.

1 Introduction

Both, CCN properties and hygroscopic growth of aerosols are determined by the amount and nature of the soluble material contained in the particles. It is therefore reasonable to assume a relationship between the hygroscopic growth at subsaturated conditions and the critical supersaturation of droplet activation. This has been the motivation for developing models to predict critical supersaturations based on aerosol hygroscopic growth factors measured at subsaturated conditions (e.g., Brechtel and Kreidenweis, 2000a; Brechtel and Kreidenweis, 2000b; Rissler et al., 2004; Kreidenweis et al., 2005; Koehler et al., 2006; Petters and Kreidenweis, 2007; Wex et al., 2008; Ziese et al., 2008, Ervens at al., 2007). Similar strategies have been used for hygroscopicity/CCN closure studies on ambient aerosols (e.g., Covert et al., 1998; Dusek et al., 2003; Gasparini et al., 2006; Vestin et al., 2007; Mochida et al., 2006; Svenningsson et al., 1997), on jet engine exhaust (Gysel et al., 2003; Hitzenberger et al., 2003), on secondary organic aerosol (Wex et al., 2009; Petters et al., 2009), and on laboratory-generated coated soot particles (Henning et al., 2010; Snider et al., 2010; Stratmann et al., 2010). In addition, there has been one study comparing hygroscopic growth and CCN activation of biomass burning aerosol (Petters et al., 2009). These closure studies have had various degrees of success, but in principle it can be concluded that predicting CCN properties based on hygroscopic growth factors is similarly or more successful than predicting CCN properties based on chemical information.

One important reason for a potential failure of the extrapolation from hygroscopic growth measurements to CCN properties is the presence of slightly soluble (SS) or surfactant (SA) organic compounds in the aerosol. These organic compounds influence in different manner the water uptake at sub- and at supersaturated conditions. SS substances contribute little to the water uptake at subsaturated conditions, because they do not fully dissolve even at high relative humidities (RH) in the concentrated solution droplets. Their contribution to the water uptake is larger at supersaturated conditions because more of the SS material dissolves in the diluted droplets. Changes in surface

Water uptake of biomass burning aerosol

U. Dusek et al.

tension due to SA substances barely affect the water uptake at subsaturated conditions. However, a decrease in droplet surface tension near the critical supersaturation greatly facilitates CCN activation (Facchini et al., 1999). In both cases the particles are more easily activated to cloud droplets than would be expected based on the water uptake at RH below 100%.

Little is known about the importance of SS and SA substances for CCN activation in the atmosphere. In some environments, the comparison of measured CCN concentrations with CCN concentrations predicted from hygroscopic growth factors has suggested that the influence of SA and SS substances is limited (e.g., Dusek et al., 2003; Gasparini et al., 2006; Ervens et al., 2005; Andreae and Rosenfeld, 2008). However, where the aerosol composition is dominated by organic material, there is an indication that compounds of limited solubility cause discrepancies in the water uptake at sub- and supersaturated conditions (Mircea et al., 2005; Mochida et al., 2006).

In the present study we aim to investigate the possible presence of SA and SS substances in fresh biomass burning emissions and their importance for CCN activation. We identify such substances indirectly, by investigating possible discrepancies in the water uptake at sub- and supersaturated conditions. Such a comparison of water uptake requires precise information on hygroscopic growth and critical supersaturations of the aerosol particles. This study therefore greatly benefits from size-resolved CCN spectra (Frank et al., 2006) measured at the same dry particle diameters (d_p) as the corresponding hygroscopic growth factors (GF).

2 Experimental methods

The properties of pyrogenic aerosols were studied as part of the project EFEU (Wurzler et al., 2001) in the combustion laboratory in Mainz, which is described in detail by Iinuma et al. (2006). The laboratory fires were sustained on a fuel bed housed in a container open to the ambient air. Through an exhaust stack, the smoke was drawn into a continuous-flow mixing chamber, from which the aerosol was sampled. The

duration of each experiment was approximately one hour and included both flaming and smoldering conditions, with typical excess CO/CO_2 ratios between 3 and 15%.

Size-resolved CCN spectra were measured by using a differential mobility analyzer (DMA) upstream of a static thermal gradient CCN counter (Frank et al., 2007). The DMA selected particles within a narrow size range (aerosol to sheath flow ratio of 1/10) at a relative humidity of less than 10%. These particles were then passed to the CCN counter and a condensation particle counter (CPC; TSI 3762) measuring in parallel. While the CCN counter measured the particles that were activated as CCN at a certain supersaturation S, the CPC measured the total particle number concentration (CN). The fraction of activated particles (defined as CCN/CN) was calculated for each supersaturation (S) and dry particle diameter (d_p), after correction for multiply charged particles (Frank et al., 2006; Rose et al., 2008).

For chemical analysis, particles were sampled using a Berner-type cascade impactor (Berner and Lürzer, 1987). The deposited material on each stage was quantitatively analyzed with respect to inorganic ions, apparent elemental carbon (EC_a; Andreae and Gelencsér, 2006), organic carbon (OC), water soluble organic carbon (WSOC), and water insoluble organic carbon (WIOC, calculated as OC minus WSOC). The methods used were ion chromatography for inorganic ions, a thermographic method for OC/EC_a (VDI, 1999), and a Shimadzu TOC analyzer for WSOC. A more detailed description of the impactor measurements can be found in Iinuma et al. (2006).

Measurements of particle hygroscopic growth were done using a Hygroscopicity-Tandem Differential Mobility Analyzer (H-TDMA). The H-TDMA consists of two Differential Mobility Analyzers (DMA1 and DMA2) separated by a conditioning unit where the particles are exposed to an elevated relative humidity RH < 100%. DMA1 selects a nearly monodisperse fraction of the aerosol, while DMA2 scans the humidified size distribution after the conditioning unit. The raw humidified size distribution is inverted using an algorithm by Voutilainen et al. (1999) and the hygroscopic growth factor (GF) is defined as the ratio of the median wet particle diameter determined by DMA 2 and the dry particle diameter (d_p) determined by DMA 1.

3   Data analysis methods

Discrepancies in the water uptake based on model calculations at subsaturated and supersaturated conditions can give an indication for the presence of SA and/or SS material. An efficient tool for detecting such inconsistencies is calculating so-called equivalent soluble volume fractions (ε). Soluble volume fractions have been used in the past, mainly to parameterize hygroscopic growth measurements (e.g., Swietlicki et al., 1999; Lehmann et al., 2005; and references therein). They are calculated based on a hypothetical model particle that is only composed of insoluble material surrounded by a model solute, often ammonium sulfate. The parameter ε is defined as the volume fraction of model solute compared to the total particle volume, which can explain the observed water uptake. More recently, other parameterizations have been suggested (e.g., Rissler et al., 2004), of which the most widely used is the κ-parameterization of Petters and Kreidenweis (2007). These parameterizations are equivalent e.g., κ can be expressed in terms of the soluble volume fraction as $\kappa = \varepsilon \cdot \kappa_m$, where κ_m is the hygroscopicity parameter of the model salt. Because of the widespread use of κ we will express some of our main results also in terms of κ, using $\kappa_m = 0.6$ for ammonium sulfate.

In this work, we calculate ε both from measured growth factors (ε_G) and CCN spectra (ε_{CCN}) using ammonium sulfate as the model salt. If these volume fractions show only small differences typical of non-idealities of model salt and particle constituents, this indicates that there is no large influence of SS and SA substances. If ε_{CCN} is substantially larger, SS or SA substances are probably present affecting the activation behavior of the particles.

3.1 Calculating ε_G

ε_G can be estimated from the water uptake of a particle at RH < 100% using an approach similar to Dusek et al. (2003):

$$\varepsilon_G = \frac{V_s}{V_{dry}} = \frac{\eta(RH) \cdot m_w(RH) \cdot M_s}{\rho_s \cdot V_{dry}}, \tag{1}$$

where V_s is the volume of the model solute, V_{dry} the volume of the dry particle, η the molality of the solution at the given RH, m_w the mass of water taken up by the particle at the given RH, ρ_s the density, and M_s the molecular weight of the model substance.

Assuming volume additivity and particle sphericity, m_w can be calculated from the measured diameter growth factor (GF):

$$m_w(RH) = \frac{\pi \cdot d_{dry}^3 \cdot \left(GF^3(RH) - 1\right) \cdot \rho_w}{6}. \tag{2}$$

The value of $\eta(RH)$ depends on the chosen model substance. For an ideal solute, η is given by:

$$\eta = \frac{1 - a_w}{i_s \cdot M_w \cdot a_w}, \tag{3}$$

where i_s is the Van't Hoff factor of the solute and M_w is the molecular weight of water. The water activity a_w of the small solution droplet can be calculated as:

$$a_w = RH \cdot \exp\left(-\frac{4 \cdot \sigma \cdot M_w}{\rho \cdot R \cdot T \cdot GF \cdot d_{dry}}\right), \tag{4}$$

where σ and ρ are the surface tension and density of the solution, respectively. For a non-ideal solute (such as ammonium sulfate), empirical parameterizations of η as a function of the water activity can be used (see e.g., Swietlicki et al., 1999) instead of Eq. (3). Combining Eqs. (1–4), the equivalent soluble volume fraction of the model

particle can be calculated based on measured hygroscopic growth factors of the real particles with unknown composition.

3.2 Calculating ε_{CCN}

The Köhler equation for a particle consisting of a single solute and an insoluble core can be expressed in terms of the dry particle volume (V_{dry}) and the volume of the model solute (V_s).

$$S \approx \frac{A}{d} - \frac{B}{d^3 - (V_{dry} - V_s) \cdot 6/\pi}, \tag{5}$$

where d is the ambient droplet diameter. For a given model solute, A and B are constants defined below. For a given solute and dry particle size, S depends on two variables, d and the volume of the model solute V_s. The critical supersaturation S_c is defined as the maximum of the Köhler curve with respect to d:

$$S_c = \max_d(S) \tag{6}$$

and is therefore only a function of V_s. Assume now that S_c^m is the experimentally determined critical supersaturation of an actual particle with unknown composition. The volume of model solute that is consistent with S_c^m is calculated by numerically solving the following equation for V_s:

$$S_c(V_s) = S_c^m. \tag{7}$$

Finally, the equivalent soluble volume fraction is given as:

$$\varepsilon_{CCN} = V_s/V_{dry}. \tag{8}$$

The constants A and B in Eq. (5) are defined as:

$$A = \frac{4\sigma \cdot M_w}{R \cdot T \cdot \rho_w} \quad and \quad B = \frac{i \cdot 6 \cdot \rho_s \cdot M_w}{\pi \cdot M_s \cdot \rho_w}, \tag{9}$$

Title Page

Abstract | Introduction

Conclusions | References

Tables | Figures

◄◄ | ►►

◄ | ►

Back | Close

Full Screen / Esc

Printer-friendly Version

Interactive Discussion

where σ is the surface tension of the solution (strictly speaking σ depends on η and hence on i), R is the universal gas constant, T is the absolute ambient temperature, M denotes molecular mass, ρ density and the subscripts s and w stand for model solute and water, respectively. The factor i is the so-called van't Hoff factor. For ideal solutions, i is simply the number of ions into which the solute can dissolve. Solution non-ideality can be taken into account by letting the van't Hoff factor vary with the concentration of the solution. When using ammonium sulfate as a model solute we vary the van't Hoff factor according to a parameterization by Young and Warren (1994) based on data of Low et al. (1974):

$$i = -0.007931 \cdot \log(\eta)^2 - 0.18844 \cdot \log(\eta) + 1.9242 \text{ for } \eta < 1$$
$$i = 0.021 \cdot \eta^2 - 0.0428 \cdot \eta + 1.9478 \text{ for } \eta > 1 \tag{10}$$

3.3 Estimating ε_G and ε_{CCN} from measured growth distributions and CCN spectra

The Eqs. (1–10) can be used for calculating ε of monodisperse particles with well defined GF and S_c. However, for laboratory-generated biomass burning aerosol as considered here, particles of the same size do not necessarily have the same chemical composition and shape. As a consequence, biomass burning particles of a certain size class show a distribution of hygroscopic growth factors instead of a single growth factor, and gradual CCN activation spectra that are not simply represented by step functions. The derivation of the appropriate ε is therefore not straightforward.

Figure 1 shows a typical example of humidified size distributions of particles with dry diameters of $d_p = 50$, 100, and 150 nm as measured by the H-TDMA at RH = 85%. Usually, monomodal growth distributions are summarized by a single diameter growth factor GF, defined as the modal diameter of the wet size distribution divided by the centroid dry diameter. Since the hygroscopic growth factor and the soluble volume fraction are nearly linearly related, the mode of the growth factor distribution roughly corresponds to the mode of the soluble volume distribution. The distributions are fairly

(though not completely) symmetrical and as a consequence the mode, mean, and median diameter are close to each other. Therefore the experimentally determined GF can be used to calculate the soluble volume fraction ε_G that is representative for the mean soluble volume of the selected size fraction.

5   The derivation of ε_{CCN} from actual CCN spectra is not straightforward, as demonstrated on a representative example shown in Fig. 2a. For a certain particle size fraction, a typical median supersaturation S_c^m is usually derived by finding the supersaturation where 50% of the particles are activated (CCN/CN ratio = 0.5). In most cases, the CCN spectra are interpolated to find S_c^m. This supersaturation can subsequently
10   be converted to a soluble volume fraction $\varepsilon(S_c^m)$, by use of Eqs. (5–10). A different way of deriving a representative soluble volume fraction from the CCN spectra is to convert each S in the spectrum to a soluble volume fraction ε and to plot CCN/CN values as a function of ε (see Fig. 2b). Then ε_{CCN} can be calculated as the value at CCN/CN = 0.5, as indicated by the dotted vertical line in Fig. 2b. Due to the strongly nonlinear dependence of S_c on ε and the low resolution of the gradual activation curves, ε_{CCN} is roughly
15   20% larger than $\varepsilon(S_c^m)$, but still within the error bounds of our method (see Sect. 3.4). Since ε_G closely represents the median soluble volume fraction, we choose the latter method for estimating ε_{CCN}. However, this example illustrates to which extent errors related to the interpolation methods of the CCN spectra can affect the comparison of
20   ε_{CCN} and ε_G.

3.4 Error analysis

Uncertainties in the H-TDMA measurements are dominated by uncertainties in RH. The system uncertainty in RH was determined by generating sodium chloride particles at regular intervals during the lab study and comparing their hygroscopic growth with
25   theory. The calibration revealed that the system RH was stable within ±2% RH. The relative uncertainty in hygroscopic growth factor GF for a sodium chloride particle at 85% ± 2% RH is roughly ±3.5%. Because the biomass burning particles are much less hygroscopic than pure sodium chloride particles, the relative uncertainty of the

Water uptake of biomass burning aerosol

U. Dusek et al.

Title Page

Abstract | Introduction

Conclusions | References

Tables | Figures

◄◄ | ►►

◄ | ►

Back | Close

Full Screen / Esc

Printer-friendly Version

Interactive Discussion

presented data is expected to be ≤2%. The diameter growth factors measured in this study typically varied between GF = 1.04 and 1.1 (at RH = 85%). A relative uncertainty of 1% in diameter growth factor translates to relative uncertainties in ε of roughly 25% for GF = 1.04 and 10% for GF = 1.1. A relative uncertainty of 2% in diameter growth factor translates to 40% in ε for GF = 1.04 and 20% in ε for GF = 1.1. Since the uncertainties due to RH control in the instrument decrease with decreasing growth factor, a relative uncertainty of 1% seems realistic for GF in the range of 1.04. Thus an overall relative uncertainty of roughly 25% is assumed for ε_G in this study.

The method of estimating uncertainties in ε_{CCN} is illustrated in Fig. 2. The error bars (1 standard deviation) in Fig. 2a show the propagated uncertainty in CCN/CN ratios and S of a typical mean CCN spectrum (average over four individual CCN spectra taken at different times during the 1-h oak burning experiment). For some experiments, only three spectra were averaged, and in these cases the uncertainties are slightly larger. An upper bound to the spectrum is estimated using CCN/CN + δCCN/CN and $S - \delta S$, a lower bound by using CCN/CN $-\delta$CCN/CN and $S + \delta S$ (grey circles). $S - \delta S$ and $S + \delta S$ are converted to the respective upper and lower bounds of ε, which combined with the respective uncertainties in CCN/CN result in the grey curves shown in Fig. 2b. The uncertainty of ε_{CCN} is estimated by finding CCN/CN = 0.5 for each of these curves. For the oak experiment, this leads to uncertainty bounds for ε_{CCN} of [0.09, 0.16] or roughly 30%, which represents a typical uncertainty for the other biomass burning experiments as well.

3.5 The effect of particle shape on ε_{CCN} and ε_G

In this study, both the hygroscopic growth and the CCN activation are measured on particles pre-selected by a DMA according to their electrical mobility. These particles are assigned to a mobility equivalent diameter (d_m). The mobility diameter of non-spherical particles is larger than their volume equivalent diameter (d_{ve}). This has consequences for both CCN and diameter growth measurements and the calculation of ε.

The critical supersaturations derived from CCN measurements are an intrinsic property of the particles studied and do not depend on the equivalent particle diameter we use to describe the selected particles. However, the dry particle diameter is subsequently used in calculating ε_{CCN}. A larger particle requires a smaller soluble volume fraction and therefore a lower ε to be activated at the same S_c than a smaller particle. ε_{CCN} calculated based on d_m is therefore smaller than ε_{CCN} based on d_{ve}, which actually is the equivalent diameter more directly related to CCN activity.

For growth factor measurements the situation is slightly different. The hygroscopic growth factor GF itself is defined as the ratio of the wet and dry diameter. If sufficient amounts of water condense on the particles, the wet particles are spherical and as a consequence their d_m and d_{ve} are equal. For the dry particles, however, d_m can be larger than d_{ve} depending on the particle shape. Since GF is operationally defined as the ratio of wet and dry mobility diameter, it may underpredict the actual volume of water condensed on the particle, and therefore underpredict the soluble volume fraction.

The fact that the effective soluble volume fractions depend on the equivalent diameter used to describe the non-spherical particles does not necessarily limit their usefulness. Soluble volume fractions are only a simplified model to parameterize the water uptake of aerosol particles and if they are used together with the diameter for which they are derived, they will give correct results for S_c and GF. However, for irregular particles of the same chemical composition, ε_G and ε_{CCN} can be different, even without surface tension effects or the influence of slightly soluble material. This could therefore lead to incorrect interpretations of our measurements. The biomass burning particles produced in the EFEU chamber appear as compact clusters of small spherules in the SEM (Dusek et al., 2004). They are not chain-like or highly fractal in nature and their shape factors have been determined to be <1.2 (Schneider et al. 2006), but could still exceed 1.

Table 1 summarizes the influence of the shape factor ($X = d_m/d_{\text{ve}} \cdot C_c(d_{\text{ve}})/C_c(d_m)$, where C_c is the Cunningham slip correction factor) on ε_G and ε_{CCN}, for a particle

Water uptake of biomass burning aerosol

U. Dusek et al.

Title Page

Abstract	Introduction
Conclusions	References
Tables	Figures

◄ ►

◄ ►

| Back | Close |

Full Screen / Esc

Printer-friendly Version

Interactive Discussion

composed of 30% levoglucosan and 70% insoluble material, assuming a mobility diameter of $d_m = 100$ nm is selected by the DMA. The second column in Table 1 shows the decrease in d_{ve} with increasing shape factor. The equilibrium wet diameter (d_{wet}) is calculated using Eqs. (11–12) and the respective d_{ve}. The measured hygroscopic growth factor GF, defined as d_{wet}/d_m, decreases strongly with increasing X. Since the critical supersaturation depends inversely on the amount of soluble material in the particle, it increases with decreasing d_{ve}. However, the resulting reduction in ε_{CCN} is much more moderate than the reduction in ε_G. We can deduce from his example that slight variations in shape factor cause a larger variation in ε_G than ε_{CCN}.

4 Sensitivity studies

Before analyzing the experimental data we need to evaluate the method of detecting SS and SA substances via comparison of ε_{CCN} and ε_G:

i. Is this method very sensitive to the model substance we choose to calculate ε? I.e., does potential non-ideal behavior in the model salt lead to large differences in ε_G and ε_{CCN}, without any presence of SA or SS substances?

ii. How sensitive is this method to the effects of SS and SA substances? I.e., how much of surface tension suppression and what amount of slightly soluble material will lead to a significant difference in ε_G and ε_{CCN}?

4.1 Non-ideal effects of ammonium sulfate as a model salt

The extent to which non-idealities of ammonium sulfate influence the calculation of ε depends on the unknown composition of the analyzed particle. The magnitude of this effect can be assessed by applying the method to a droplet that behaves as an ideal solution. As an example we consider an idealized biomass burning particle consisting of 30% levoglucosan and 70% insoluble material. Previous laboratory studies

have shown that the water uptake of levoglucosan at sub- and supersaturations can be roughly approximated by that of an ideal solute with a van't Hoff factor of 1 (Mochida and Kawamura, 2004; Svenningsson et al., 2006). For the purpose of this sensitivity study, the weak effect of levoglucosan on surface tension at high solute concentrations (e.g., Svenningsson et al., 2006) is ignored.

First, we calculate the critical supersaturation and hygroscopic growth of the idealized biomass burning particle using the Köhler equation:

$$RH = a_w \cdot \exp\left(\frac{4 \cdot \sigma \cdot M_w}{\rho_w R \cdot T \cdot d}\right) \tag{11}$$

with

$$a_w = \frac{1}{1 + i M_w \eta} \tag{12}$$

by numerically solving Eq. (11) for the interstitial diameter d (and hence GF) at RH = 0.9, and by solving for the maximum to get S_c. The values of S_c and GF are summarized in Table 2 for several relevant particle diameters at a temperature of 293 K.

For each particle diameter, we derive ε_G and ε_{CCN} as described in Sects. 3.1 and 3.2, using ammonium sulfate as a model salt. As the model particle does not contain any slightly soluble or surface active compounds, the values of ε_G and ε_{CCN} should agree. The actual small differences (see Table 2) between the derived values of ε are due to the non-idealities of the ammonium sulfate solution. The actual biomass burning particles analyzed in later sections are not necessarily ideal solutes, but the values presented in Table 2 give a good example of the magnitude of the difference between ε_{CCN} and ε_G that can generally be expected to arise from solution non-idealities.

In order to be detected, the differences in ε_{CCN} and ε_G caused by SA and SS compounds have to be substantially larger than the differences caused by potential solution non-idealities. In the next section we estimate the sensitivity of our method to SA and SS substances and the magnitude of surface tension depression or the mass fraction of slightly soluble substances that we are able to resolve.

4.2 Sensitivity of ε to surface tension depression

The sensitivity of ε_{CCN} to SA compounds can be studied by artificially reducing the surface tension of the idealized biomass burning particle to 90% and 80% of the value of pure water. This reduces the critical supersaturation of the particle as shown in Table 3, and as a consequence increases ε_{CCN}. The increase in the value of ε_{CCN}, which is independent of particle diameter, was calculated using both ammonium sulfate and levoglucosan as model substances, to compare their respective usefulness as a model substance. The initial value of the effective ε_{CCN} at the surface tension of water is much lower when ammonium sulfate is used as a model substance (0.10) than when levoglucosan is used (0.30). Table 3 shows that reducing the surface tension by 20%, results in a doubling of the effective ε_{CCN} for both model substances. Using the κ notation eliminates the complication introduced by the choice of a model substance, as the hygroscopicity, κ, of the model aerosol is simply calculated as $\kappa_{CCN} = \kappa_{LGS} \cdot V_{LGS}/V_{dry}$, where LGS stands for levoglucosan, and $\kappa_{LGS} = 0.21$ (Petters and Kreidenweis, 2007). The initial κ_{CCN} value of the model aerosol is thus 0.06, and increases to 0.12 when the surface tension is reduced by 20%.

ε_G (or κ_G) is not influenced by a change in surface tension and remains at 0.11–0.12 for ammonium sulfate (Table 2) and 0.3 for levoglucosan, since the Kelvin effect is small for particles larger than 50 nm as considered here (see Eq. 4, exponential term). We can therefore conclude that a surface tension reduction of more than 10% results in a larger difference between ε_{CCN} and ε_G than would be expected from non-ideal solution effects. Therefore we are able to resolve moderate changes in surface tension (larger than 10%) by comparing ε_{CCN} and ε_G.

Despite the fact that levoglucosan (as the main molecularly identified organic component of fresh biomass burning aerosol) might seem the model substance of choice, Table 3 shows that it is not suited to detect large changes in surface tension, since the effective soluble volume fractions would exceed 1. The same is true for analyzing particles that contain a significant fraction of inorganic ions, such as particles released by

the burning of grass (Iinuma, 2006). Therefore, we decided to use ammonium sulfate as a model substance in the analysis presented in this work.

4.3 Sensitivity of ε to slightly soluble substances

Slightly soluble substances alter the expected critical supersaturation most drastically if they are virtually undissolved at subsaturated conditions, but fully dissolved at supersaturated conditions near S_c. We choose succinic acid as an example of a SS substance, due to its moderate solubility of 88 g/l (Saxena and Hildemann, 1996). The moderate reduction in surface tension due to succinic acid at high solution concentrations was ignored for the following sensitivity study to focus solely on the solubility effect.

We calculated critical supersaturations and hygroscopic growth factors for a particle consisting of levoglucosan and succinic acid in varying proportions using the form of the Köhler equation as written in Eq. (11), but with

$$a_w = \frac{1}{1 + \frac{6M_w m_l}{\pi M_l \rho_w \left(d^3 - d_{dry}^3\right)} + \frac{M_w sol}{M_{ss} \rho_w}} \tag{13}$$

when succinic acid is not completely dissolved and

$$a_w = \frac{1}{1 + \frac{6M_w}{\pi \rho_w \left(d^3 - d_{dry}^3\right)} \left(\frac{m_l}{M_l} + \frac{m_{ss}}{M_{ss}}\right)} \tag{14}$$

when succinic acid is completely dissolved. The term sol is the solubility of succinic acid in g/l. The subscript w denotes water, l denotes levoglucosan and ss the slightly soluble substance (in this case succinic acid). Van't Hoff factors of 1 are assumed for both levoglucosan and succinic acid.

S_c and GF of the model particles are summarized in Table 4. The critical supersaturations are not strongly affected by the increasing mass fractions of succinic acid as a

consequence of similar density and molecular weight of succinic acid and levoglucosan and the fact that succinic acid is nearly fully dissolved at the point of activation. The hygroscopic growth factors, however, decrease drastically (from about 1.13 to 1.05) when levoglucosan is replaced by the nearly undissolved succinic acid at RH = 90%.

Table 5 shows effective soluble volume fractions calculated from S_c and GF in Table 4. For pure levoglucosan particles ε_G and ε_{CCN} are similar, but with increasing succinic acid fractions, ε_G is reduced to roughly 1/2 and 1/5 of ε_{CCN}. Therefore, we conclude that we can detect significant fractions of slightly soluble material with reasonable accuracy applying our model.

5 Results

We analyzed nine of the wood burning experiments, comprising all experiments for which both hygroscopic growth factors and CCN spectra were available. These included two experiments burning hardwood fuels (oak and musasa), three experiments burning softwood fuels (pine and spruce) and four experiments burning softwood fuels along with fresh or dry branches and needles. Chemical analyses of impactor samples (Iinuma et al., 2007) were available for six of those experiments. Due to the limited number of experiments available, we sometimes added additional data from a pre-experiment, which are specifically identified in each section or graph.

Figure 3 shows grand averages of ε_G and ε_{CCN}, using ammonium sulfate as a model salt. ε of freshly emitted wood burning aerosol is generally small, corresponding to a particle containing roughly 10% ammonium sulfate and otherwise insoluble material. Table 6 summarizes these average values of ε together with the widely used κ-parameterization of particle hygroscopicity. The κ values from our experiment compare well to the range of κ-values (0.05–0.2) obtained by Petters et al. (2009) for similar fuel types (i.e., wood or branches with needles or leaves). Petters et al. (2009) found that grasses and other materials such as sugar cane or rice straw were generally more hygroscopic, which was also noted during our experiment (Janhäll et al., 2010).

Although individual values of ε have large uncertainties, the averages over many experiments agree well for 100 and 150 nm. However, for 50 nm particles, ε_{CCN} and ε_G differ significantly at the 95% confidence level. Moreover, ε_{CCN} and ε_G show opposing trends with particle size. ε_{CCN} increases linearly with decreasing particle diameter,
5 whereas ε_G is similar for 100 and 150 nm particles but decreases somewhat for 50 nm particles. Petters et al. (2009) also observed good agreement between κ derived from hygroscopic growth factors and CCN spectra around the 100 nm size range. However, they also note an increase in hygroscopic growth factors towards smaller particle sizes that we did not observe in this study.

10 An increase in ε_{CCN} with decreasing size would be consistent with the possibility that smaller particles contain more soluble material. This could be expected, if soluble material condenses on pre-existing soot cores during the cooling of the vaporized material. However, in this case ε_G should increase as well, and therefore the decrease in ε_G at 50 nm renders this hypothesis relatively unlikely. An increase in soluble material
15 that does not increase ε_G could only be explained, if most of this material was only slightly soluble. However there is no likely reason why slightly soluble material should be enriched in 50 nm particles to such an extent.

The most likely explanation for the observed increase in ε_{CCN} without a concurrent increase in ε_G is the presence of surfactant organics. At the point of critical supersatu-
20 ration, the droplets that form by condensation on small particles are more concentrated than droplets that form on larger particles. The surface tension of surfactant solutions tends to decrease with solution concentration (e.g., Facchini et al., 2000; Svenningsson et al., 2006). Therefore, it is possible that surface active material is relatively ineffective at large particle sizes, but begins to significantly decrease the critical supersaturation
25 for small particles.

Figure 4 presents scatter plots of ε_{CCN} versus ε_G for each particle diameter. Each data point represents an individual burning experiment of approximately one hour. Hardwood fuels (musasa, oak) are indicated as black squares, softwood fuels (spruce, pine) as white circles, and softwood fuels including needles and branches as grey

triangles. For 150 nm particles we display additional data from a pilot study conducted in spring 2003. These data are not included in the grand averages presented in Fig. 3, because both diameter growth factors and critical supersaturations tended to be lower than in the fall experiment due to different burning conditions. The error bars show the respective experimental uncertainties in ε (see Sect. 3.4). At 50 nm the difference between ε_G and ε_{CCN} is clearly outside the range that could be explained by experimental uncertainties.

Individual values of ε_{CCN} and ε_G are not strongly correlated. This is partially due to the limited range of ε values and to the large experimental uncertainty, which results in significant scatter of the data points. However, the experimental uncertainties cannot explain all the variability and lack of correlation in the data set. Another part of the variability is probably due to the fact that CCN and growth factor measurements did not take place at exactly the same times during each experiment. Furthermore, there is a systematic difference in variability between ε_{CCN} and ε_G. Despite comparable experimental uncertainties, the ε_G data have roughly twice the relative standard deviation of the ε_{CCN} data. Moreover, the correlation between ε_G at 50 nm and ε_G at 100 nm particles is poor ($R^2 = 0.29$), whereas ε_{CCN} of 50 and ε_{CCN} of 100 nm particles are tightly correlated ($R^2 = 0.90$). This means that in fuels where 50 nm particles were easily activated, 100 nm particles were easily activated as well, whereas at subsaturated conditions there does not seem to exist a clear relationship between the hygroscopicity of the 50 and 100 nm particles.

The large scatter in growth factor data could be caused by the shape of the biomass burning particles. As demonstrated in Sect. 3.5 even relatively small deviations from spherical shape (shape factors between 1 and 1.2) can have a large effect on ε_G. There is also the possibility of restructuring upon water condensation. Both effects reduce the measured hygroscopic growth factor and could cause additional variability in ε_G.

In Fig. 5, ε_G and ε_{CCN} are compared to volume fractions of soluble material estimated from impactor samples (Iinuma et al., 2007). For this comparison, we used the first impactor stage, which had aerodynamic cut-off diameters of 50 and 150 nm.

This corresponds to 36 and 125 nm volume equivalent diameters, assuming a density of 1600 kg m^{-3} for the biomass burning particles or to 44 and 140 nm using a density of 1200 kg m^{-3}. The black bars represent volume fractions of inorganic ions and the grey bars represent volume fractions of water soluble organic carbon ε_{WSOC}. These volume fractions are rough estimates using densities of 1700 kg m^3 for the inorganic fraction, 2000 kg m^{-3} for elemental carbon, 1400 kg m^{-3} for the organic fraction, and 1500 kg m^{-3} for the unresolved material. Both ε_G (squares) and ε_{CCN} (triangles) are volume-weighted averages of the individual ε derived for 50 and 100 nm particles.

The water soluble fraction of the first impactor stage is dominated by organic material, while volume fractions of inorganic ions are low for all wood burning experiments. ε_G and ε_{CCN} are much larger than the volume fractions of inorganic ions. Since ε denotes the inorganic volume fractions (here represented by ammonium sulfate) that explain the observed water uptake, this is a clear indication that the organic material must be responsible for most of the water uptake in fresh biomass burning aerosol. On the other hand, ε is consistently smaller than the WSOC volume fraction, indicating that the organics are not as efficient in water uptake as ammonium sulfate.

Based on this comparison, it is possible to give a crude estimate of the effectiveness of the WSOC fraction with respect to water uptake. Assuming that the water uptake of the inorganic fraction is of a similar order of magnitude as that of ammonium sulfate, we subtract ε_{ion} from ε_{CCN} and ε_G. The remainder gives the part of ε that is not explained by the water uptake of inorganics and therefore represents the water uptake of the WSOC fraction. More specifically it gives the volume fraction of ammonium sulfate that attracts a comparable amount of water as the observed WSOC fraction. The ratio of $(\varepsilon_G - \varepsilon_{ion})/\varepsilon_{WSOC}$ is roughly 1/3, whereas the ratio of $(\varepsilon_{CCN} - \varepsilon_{ion})/\varepsilon_{WSOC}$ is roughly 1/4. This indicates that the organics take up roughly 1/3 to 1/4 of the water that a comparable amount of ammonium sulfate would take up. As a rule of thumb the water uptake of fresh biomass burning particles can be approximated by representing 1/3 to 1/4 of the WSOC by ammonium sulfate and assuming the rest of the carbonaceous material to be inactive. In the κ-formulation this would mean that the water-soluble

organic material can be represented by a κ value of 0.15–0.20, which is higher than the κ value of ~0.1 suggested for fresh secondary organic aerosol (e.g., Dusek et al., 2010; Petters and Kreidenweis, 2007). The effective hygroscopicity of the total aerosol material can then be represented by a linear mixture of an inorganic component with $\kappa \cong 0.6$, a WSOC component with $\kappa \cong 0.18$, and an insoluble component with $\kappa = 0$.

6 Discussion

6.1 The role of surfactants

The presence of SA substances is a possible explanation for the increase of ε_{CCN} with decreasing particle size and for the difference between ε_{CCN} and ε_G at 50 nm. Iinuma et al. (2007) show that the pyrogenic particles studied during the EFEU experiment contained a significant amount of macromolecules. While the nature of these macromolecules is not entirely certain, it has been shown previously (e.g., Facchini et al., 2000; Dinar et al., 2006; Fors et al., 2009), that macromolecular substances such as humic like substances (HULIS) can have a strong effect on droplet surface tension.

It is known in principle that SA substances cause an apparent increase in ε_{CCN} with decreasing particle size, since an equal fraction of surfactant is more concentrated in solution droplets forming on small particles. However, it still needs to be explored, whether a realistic SA substance can account for the observed increase in S_c solely due to the concentration effect. Therefore, we conducted a sensitivity study, considering an idealized biomass burning particle with a composition of 30% levoglucosan, 5% fulvic acid and 65% insoluble material. The dependence of droplet surface tension on fulvic acid concentration is parameterized according to Svenningsson et al. (2006). Table 7 shows that even though particles of 50, 100, and 150 nm contain the same fraction of surfactant, the surface tension of the droplet at S_c decreases with decreasing dry particle diameter. The resulting increase of ε_{CCN} of the model particle is comparable to that observed with the actual biomass burning particles (Fig. 3).

This sensitivity study shows that a small amount of surfactant similar to fulvic acid could cause the observed increase in ε_{CCN} with decreasing particle diameter and the resulting difference in ε_{CCN} and ε_G. This strengthens the evidence that surfactants modify the CCN activation of fresh biomass burning particles at small particle sizes.

6.2 Water interaction in relation to chemical speciation

Figure 5 strongly suggests that the water uptake of fresh biomass burning particles is mainly governed by organic material, with only a small contribution from inorganic compounds. The organic fraction of fresh biomass burning particles is strongly soluble and takes up roughly 1/3–1/4 of the water of a comparable volume of ammonium sulfate. This is only possible if the organic fraction consists on average of relatively small molecules. These results fit well with observations that levoglucosan is by far the dominant individual organic component of fresh biomass burning aerosol (Iinuma et al., 2007). Levoglucosan has a similar molecular weight and density as ammonium sulfate, but a smaller van't Hoff factor around 1 (Mochida and Kawamura, 2004), instead of roughly 2.3–3. Assuming the WSOC fraction to consist of pure levoglucosan predicts water uptake that slightly overestimates the measured water uptake. This could be due to irregular particle shapes (see Table 3). Another possibility is that the presence of macromolecules as detected by Iinuma et al. (2007) increases the mean molecular mass of the water soluble fraction. However, considering the high uncertainties associated with estimating WSOC fractions from impactor measurements, approximating the WSOC fraction with levoglucosan leads to a reasonable estimate of S_c.

6.3 Atmospheric relevance

In this study, we find indications for an enhancement of CCN activation due to a possible decrease in droplet surface tension as proposed by Facchini et al. (1999). For our fresh biomass burning particles, this effect only begins to be important at dry particle sizes of around 50 nm, for which the solution droplets are sufficiently concentrated

at their critical supersaturation. However, the 50 nm particles typically require supersaturations of 1% or above for activation, and are therefore not very important CCN under atmospheric conditions and ambient particle size distributions, where usually a considerable number of larger particles is also present. For lower supersaturations,
5 more typical of ambient clouds, the surface tension does not strongly affect the CCN properties. The critical supersaturations of fresh biomass burning particles can then be predicted reasonably well from the known water uptake at subsaturated conditions, even using such a simple model salt as ammonium sulfate.

    As particles age in the biomass burning plumes, they acquire more water soluble
10 material through photochemical processes. Decesari et al. (2006) found that in ambient aerosol during the Amazon biomass burning season, levoglucosan was only one constituent among many, such as mono/-dicarboxylic acids, sugars, sugar-alcohols, polyhydroxylated species and others. Humic like substances can become further enriched due to polymerization processes (Kalberer et al., 2004). For these aged biomass
15 burning particles, slightly soluble material might be present and surface tension effects might be stronger, so that the simple ammonium sulfate model might not be appropriate any more. This might be the reason why Rissler et al. (2004) needed a more complex model to successfully predict CCN concentrations from size distributions and hygroscopic diameter growth factors.

20 **7 Conclusions**

We derived effective soluble volume fractions of freshly emitted biomass burning particles from size-resolved hygroscopic diameter growth factors (ε_G) and CCN spectra (ε_{CCN}) using ammonium sulfate as a model salt. The ε values of freshly emitted biomass burning particles are small, ranging between 0.05 and 0.2. This means that
25 the water uptake of the biomass particles is equivalent to particles consisting of 5–20% ammonium sulfate and otherwise insoluble material. The fraction of inorganic ions in impactor samples of the biomass burning particles is much smaller than 5–20%, indicating that the water uptake is mainly governed by organic material.

One main emphasis of this study was to compare ε_G and ε_{CCN} to gain information about the possible influence of surface active or slightly soluble substances on CCN activation. Sensitivity studies show that unless surface active or slightly soluble substances are present in the particles, the soluble volume fractions, ε_G and ε_{CCN}, should be comparable within 10%. We found a significant difference in ε_G and ε_{CCN} only for small particles of 50 nm in size, but not for particles of 100 and 150 nm in diameter. This behavior is consistent with the presence of a surfactant that facilitates droplet activation leading to a larger inferred ε_{CCN} than ε_G. Even if volume fraction of the surfactant is constant for all dry particles sizes, it will be more concentrated in deliquescent droplets that form on small particles and more diluted in droplets forming on larger particles. This explains that the effect is only visible at small particle sizes. The observed increase in ε_{CCN} with decreasing particle diameter could be reproduced with an idealized biomass burning particle consisting of 30% levoglucosan, 65% insoluble material, and 5% fulvic acid, indicating that only a small amount of surfactant is necessary for the observed effects.

References

Andreae, M. O. and Gelencsér, A.: Black carbon or brown carbon? The nature of light-absorbing carbonaceous aerosols, Atmos. Chem. Phys., 6, 3131–3148, doi:10.5194/acp-6-3131-2006, 2006.
Andreae, M. O. and Rosenfeld, D.: Aerosol-cloud-precipitation interactions. Part 1. The nature and sources of cloud-active aerosols, Earth Sci. Rev., 89, 13–41, 2008.

Berner, A. and Lürzer C.: Mass size distributions of traffic aerosols at Vienna, J. Phys. Chem. 84, 2079–2083, 1987.

Brechtel, F. J. and Kreidenweis, S. M.: Predicting particle critical supersaturation from hygroscopic growth measurements in the humidified TDMA. part I: Theory and sensitivity studies, J. Atmos. Sci., 57, 1854–1871, 2000a.

Brechtel, F. J. and Kreidenweis, S. M.: Predicting particle critical supersaturation from hygroscopic growth measurements in the humidified TDMA. Part II: Laboratory and ambient studies, J. Atmos. Sci., 57, 1872–1887, 2000b.

Covert, D. S., Gras, J. L., Wiedensohler, A., and Stratmann, F.: Comparison of directly measured CCN with CCN modeled from the number-size distribution in the marine boundary layer during ACE 1 at Cape Grim, Tasmania, J. Geophys. Res. 103, 16597–16608, 1998.

Decesari, S., Fuzzi, S., Facchini, M. C., Mircea, M., Emblico, L., Cavalli, F., Maenhaut, W., Chi, X., Schkolnik, G., Falkovich, A., Rudich, Y., Claeys, M., Pashynska, V., Vas, G., Kourtchev, I., Vermeylen, R., Hoffer, A., Andreae, M. O., Tagliavini, E., Moretti, F., and Artaxo, P.: Characterization of the organic composition of aerosols from Rondônia, Brazil, during the LBA-SMOCC 2002 experiment and its representation through model compounds, Atmos. Chem. Phys., 6, 375–402, doi:10.5194/acp-6-375-2006, 2006.

Dinar, E., Taraniuk, I., Graber, E. R., Katsman, S., Moise, T., Anttila, T., Mentel, T. F., and Rudich, Y.: Cloud Condensation Nuclei properties of model and atmospheric HULIS, Atmos. Chem. Phys., 6, 2465–2482, doi:10.5194/acp-6-2465-2006, 2006.

Dusek, U., Covert, D. S., Wiedensohler, A., Neususs, C., Weise, D., and Cantrell, W.: Cloud condensation nuclei spectra derived from size distributions and hygroscopic properties of the aerosol in coastal south-west Portugal during ACE-2, Tellus B, 55, 35–53, 2003.

Dusek, U., Frank, G. P., Helas, G. Iinuma, Y., Zeromskiene, K., Gwaze, P., Hennig, T., Massling, A., Schmid, O., Herrmann, H., Wiedensohler, A., and Andreae, M. O.: "Missing" cloud condensation nuclei in peat smoke, Geophys. Res. Lett., 32, L11802, doi:10.1029/2005GL022473, 2005.

Dusek, U., Frank, G. P., Curtius, J., Drewnick, F., Schneider, J., Kürten, A., Rose, D., Andreae, M. O., Borrmann, S., and Pöschl, U.: Enhanced organic mass fraction and decreased hygroscopicity of cloud condensation nuclei (CCN) during new particle formation events, Geophys. Res. Lett., 37, L03804, doi:10.1029/2009GL040930, 2010.

Ervens, B., Feingold, G., and Kreidenweis, S. M.: Influence of water-soluble organic carbon on cloud drop number concentration, J. Geophys. Res., 110, D18211,

Water uptake of biomass burning aerosol

U. Dusek et al.

Title Page

Abstract	Introduction
Conclusions	References
Tables	Figures

◀◀   ▶▶

◀   ▶

Back   Close

Full Screen / Esc

Printer-friendly Version

Interactive Discussion

doi:10.1029/2004JD005634, 2005.

Ervens, B., Cubison, M., Andrews, E., Feingold, G., Ogren, J. A., Jimenez, J. L., DeCarlo, P., and Nenes, A.: Prediction of cloud condensation nucleus number concentration using measurements of aerosol size distributions and composition and light scattering enhancement due to humidity, J. Geophys. Res., 112, D10S32, doi:10.1029/2006JD007426, 2007.

Facchini, M. C., Mircea, M., Fuzzi, S., and Charlson, R. J.: Cloud albedo enhancement by surface-active organic solutes in growing droplets, Nature, 401, 257–259, 1999.

Facchini, M. C., Decesari, S., Mircea, M., Fuzzi, S., and Loglio, G.: Surface tension of atmospheric wet aerosol and cloud/fog droplets in relation to their organic carbon content and chemical composition, Atmos. Environ., 34, 4853–4857, 2000.

Fors, E. O., Rissler, J., Massling, A., Svenningsson, B., Andreae, M. O., Dusek, U., Frank, G. P., Hoffer, A., Bilde, M., Kiss, G., Janitsek, S., Henning, S., Facchini, M. C., Decesari, S., and Swietlicki, E.: Hygroscopic properties of Amazonian biomass burning and European background HULIS and investigation of their effects on surface tension with two models linking H-TDMA to CCNC data, Atmos. Chem. Phys., 10, 5625–5639, doi:10.5194/acp-10-5625-2010, 2010.

Frank, G. P., Dusek, U., and Andreae, M. O.: Technical Note: Characterization of a static thermal-gradient CCN counter, Atmos. Chem. Phys., 7, 3071–3080, doi:10.5194/acp-7-3071-2007, 2007.

Frank, G. P., Dusek, U., and Andreae, M. O.: Technical note: A method for measuring size-resolved CCN in the atmosphere, Atmos. Chem. Phys. Discuss., 6, 4879–4895, doi:10.5194/acpd-6-4879-2006, 2006.

Gasparini, R., Collins, D. R., Andrews, E., Sheridan, P. J., Ogren, J. A., and Hudson, J. G.: Coupling aerosol size distributions and size-resolved hygroscopicity to predict humidity-dependent optical properties and cloud condensation nuclei spectra, J. Geophys. Res., 111, D05S13, doi:10.1029/2005JD006092, 2006.

Gysel, M., Nyeki, S., Weingartner, E., Baltensperger, U., Giebl, H., Hitzenberger, R., Petzold, A., and Wilson, C. W.: Properties of jet engine combustion particles during the PartEmis experiment: Hygroscopicity at subsaturated conditions: Geophys. Res. Lett., 30, 1566, doi:10.1029/2003GL016896, 2003.

Wex, H., Hennig, T., Kiselev, A., Snider, J. R., Rose, D., Dusek, U., Frank, G. P., Poeschl, U., Kristensson, A., Bilde, M., Tillmann, R., Kiendler-Scharr, A., Mentel, T. F., Walter, S., Schneider, J., Wennrich, C., and Stratmann, F.: Soluble mass, hygroscopic growth, and

Water uptake of biomass burning aerosol

U. Dusek et al.

droplet activation of coated soot particles during LACIS Experiment in November (LExNo), J. Geophys. Res., 115, D11206, doi:10.1029/2009JD012626, 2010.

Hitzenberger, R., Giebl, H., Petzold, A., Gysel, M., Nyeki, S., Weingartner, E., Baltensperger, U., and Wilson, C. W.: Properties of jet engine combustion particles during the PartEmis experiment. Hygroscopic growth at supersaturated conditions, Geophys. Res. Lett., 30, 1779, doi:10.1029/2003GL017294, 2003.

Iinuma, Y., Bruggemann, E., Gnauk, T., Muller, K., Andreae, M. O., Helas, G., Parmar, R., and Herrmann, H.: Source characterization of biomass burning particles: The combustion of selected European conifers, African hardwood, savanna grass, and German and Indonesian peat, J. Geophys. Res., 112, D08209, doi:10.1029/2006JD007120, 2007.

Kalberer, M., Paulsen, D., Sax, M., Steinbacher, M., Dommen, J., Prevot, A. S. H., Fisseha, R., Weingartner, E., Frankevich, V., Zenobi, R., and Baltensperger, U.: Identification of polymers as major components of atmospheric organic aerosols, Science, 303, 1659–1662, 2004.

Koehler, K. A., Kreidenweis, S. M., DeMott, P. J., Prenni, A. J., Carrico, C. M., Ervens, B., and Feingold, G.: Water activity and activation diameters from hygroscopicity data – Part II: Application to organic species, Atmos. Chem. Phys., 6, 795–809, doi:10.5194/acp-6-795-2006, 2006.

Kreidenweis, S. M., Koehler, K., DeMott, P. J., Prenni, A. J., Carrico, C., and Ervens, B.: Water activity and activation diameters from hygroscopicity data – Part I: Theory and application to inorganic salts, Atmos. Chem. Phys., 5, 1357–1370, doi:10.5194/acp-5-1357-2005, 2005.

Lehmann, K., Massling, A., Tilgner, A., Mertes, S., Galgon, D., and Wiedensohler, A.: Size-resolved soluble volume fractions of submicrometer particles in air masses of different character, Atmos. Environ., 39, 4257–4266, 2005.

Low, D. H.: A theoretical study of nineteen condensation nuclei, Journal de Recherches Atmosphériques, 4, 65–78, 1969.

Mircea, M., Facchini, M. C., Decesari, S., Cavalli, F., Emblico, L., Fuzzi, S., Vestin, A., Rissler, J., Swietlicki, E., Frank, G., Andreae, M. O., Maenhaut, W., Rudich, Y., and Artaxo, P.: Importance of the organic aerosol fraction for modeling aerosol hygroscopic growth and activation: a case study in the Amazon Basin, Atmos. Chem. Phys., 5, 3111–3126, doi:10.5194/acp-5-3111-2005, 2005.

Mochida, M. and Kawamura, K.: Hygroscopic properties of levoglucosan and related organic compounds characteristic to biomass burning aerosol particles, J. Geophys. Res., 109, D21202, doi:10.1029/2004JD004962, 2004.

Mochida, M., Kuwata, M., Miyakawa, T., Takegawa, N., Kawamura, K., and Kondo, Y.: Relationship between hygroscopicity and cloud condensation nuclei activity for urban aerosols in Tokyo, J. Geophys. Res., 111, D23204, doi:10.1029/2005JD006980, 2006.

Petters, M. D. and Kreidenweis, S. M.: A single parameter representation of hygroscopic growth and cloud condensation nucleus activity, Atmos. Chem. Phys., 7, 1961–1971, doi:10.5194/acp-7-1961-2007, 2007.

Petters, M. D., Carrico, C. M., Kreidenweis, S. M., Prenni, A. J., DeMott, P. J., Collett, J. L., and Moosmuller, H.: Cloud condensation nucleation activity of biomass burning aerosol, J. Geophys. Res., 114, D22205, doi:10.1029/2009JD012353, 2009a.

Petters, M. D., Wex, H., Carrico, C. M., Hallbauer, E., Massling, A., McMeeking, G. R., Poulain, L., Wu, Z., Kreidenweis, S. M., and Stratmann, F.: Towards closing the gap between hygroscopic growth and activation for secondary organic aerosol – Part 2: Theoretical approaches, Atmos. Chem. Phys., 9, 3999–4009, doi:10.5194/acp-9-3999-2009, 2009b.

Rissler, J., Swietlicki, E., Zhou, J., Roberts, G., Andreae, M. O., Gatti, L. V., and Artaxo, P.: Physical properties of the sub-micrometer aerosol over the Amazon rain forest during the wet-to-dry season transition - comparison of modeled and measured CCN concentrations, Atmos. Chem. Phys., 4, 2119–2143, doi:10.5194/acp-4-2119-2004, 2004.

Rose, D., Gunthe, S. S., Mikhailov, E., Frank, G. P., Dusek, U., Andreae, M. O., and Pöschl, U.: Calibration and measurement uncertainties of a continuous-flow cloud condensation nuclei counter (DMT-CCNC): CCN activation of ammonium sulfate and sodium chloride aerosol particles in theory and experiment, Atmos. Chem. Phys., 8, 1153–1179, doi:10.5194/acp-8-1153-2008, 2008.

Saxena, P. and Hildemann, L. M.: Water-soluble organics in atmospheric particles: A critical review of the literature and application of thermodynamics to identify candidate compounds, J. Atmos. Chem., 24, 57–109, 1996.

Snider, J. R., Wex, H., Rose, D., Kristensson, A., Stratmann, F., Hennig, T., Henning, S., Kiselev, A., Bilde, M., Burkhart, M., Dusek, U., Frank, G. P., Kiendler-Scharr, A., Mentel, T. F., Petters, M. D., and Pöschl, U.: Intercomparison of cloud condensation nuclei and hygroscopic fraction measurements: Coated soot particles investigated during the LACIS Experiment in November (LExNo), J. Geophys. Res., 115, D11205, doi:10.1029/2009JD012618, 2010.

Stratmann , F., Bilde, M., Dusek, U., Frank, G. P., Hennig, T., Henning, S., Kiendler-Scharr, A., Kiselev, A., Kristensson, A., Lieberwirth, I., Mentel, T. F., Pöschl, U., Rose, D., Schneider, J., Snider, J. R., Tillmann, R., Walter, S., and Wex, H.: Examination of laboratory-generated

coated soot particles: An overview of the LACIS Experiment in November (LExNo) campaign, J. Geophys. Res., 115, D11203, doi:10.1029/2009JD012628, 2010.

Svenningsson, B., Hansson, H., Martinsson, B., Wiedensohler, A., Swietlicki, E., Cederfelt, S., Wendisch, M., Bower, K., Choularton, T., and Colvile, R.: Cloud droplet nucleation scavenging in relation to the size and hygroscopic behaviour of aerosol particles, Atmos. Environ., 31, 2463–2475, 1997.

Svenningsson, B., Rissler, J., Swietlicki, E., Mircea, M., Bilde, M., Facchini, M. C., Decesari, S., Fuzzi, S., Zhou, J., Mønster, J., and Rosenørn, T.: Hygroscopic growth and critical supersaturations for mixed aerosol particles of inorganic and organic compounds of atmospheric relevance, Atmos. Chem. Phys., 6, 1937–1952, doi:10.5194/acp-6-1937-2006, 2006.

Swietlicki, E., Zhou, J. C., Berg, O. H., Martinsson, B. G., Frank, G., Cederfelt, S. I., Dusek, U., Berner, A., Birmili, W., Wiedensohler, A., Yuskiewicz, B., and Bower, K. N.: A closure study of sub-micrometer aerosol particle hygroscopic behaviour, Atmos. Res., 50, 205–240, 1999.

Vestin, A., Rissler, J., Swietlicki, E., Frank, G. P., and Andreae, M. O.: Cloud-nucleating properties of the Amazonian biomass burning aerosol: Cloud condensation nuclei measurements and modeling, J. Geophys. Res., 112, D14201, doi:10.1029/2006JD008104, 2007.

Voutilainen, A., Stratmann, F., and Kaipio, J.: A new data inversion algorithm for DMPS and TDMA measurements, J. Aerosol Sci., 30, 775–776, 1999.

Wex, H., Stratmann, F., Hennig, T., Hartmann, S., Niedermeier, D., Nilsson, E., Ocskay, R., Rose, D., Salma, I., and Ziese, M.: Connecting hygroscopic growth at high humidities to cloud activation for different particle types, Environ. Res. Lett., 3, 035004, doi:10.1088/1748-9326/3/3/035004, 2008.

Wex, H., Petters, M. D., Carrico, C. M., Hallbauer, E., Massling, A., McMeeking, G. R., Poulain, L., Wu, Z., Kreidenweis, S. M., and Stratmann, F.: Towards closing the gap between hygroscopic growth and activation for secondary organic aerosol: Part 1 – Evidence from measurements, Atmos. Chem. Phys., 9, 3987–3997, doi:10.5194/acp-9-3987-2009, 2009.

Wurzler, S., Herrmann, H., Neusüss, C., Wiedensohler, A., Stratmann, F., Wilck, M., Trautmann, T., Andreae, M. O., Helas, G., Trentmann, J., Langmann, B., Graf, H., and Textor, C.: Impact of vegetation fires on the composition and circulation of the atmosphere: Introduction of the research project EFEU, J. Aerosol Sci. 32, S199–200, 2001.

Young, K. C. and Warren, A. J.: A Reexamination of the Derivation of the Equilibrium Supersaturation Curve for Soluble Particles, J. Atmos. Sci., 49, 1138–1143, 1992

Ziese, M., Wex, H., Nilsson, E., Salma, I., Ocskay, R., Hennig, T., Massling, A., and Stratmann,

Water uptake of biomass burning aerosol

U. Dusek et al.

Title Page

Abstract	Introduction
Conclusions	References
Tables	Figures

|◄ | ►|

◄ | ►

Back | Close

Full Screen / Esc

Printer-friendly Version

Interactive Discussion

F.: Hygroscopic growth and activation of HULIS particles: experimental data and a new iterative parameterization scheme for complex aerosol particles, Atmos. Chem. Phys., 8, 1855–1866, doi:10.5194/acp-8-1855-2008, 2008.

Water uptake of biomass burning aerosol

U. Dusek et al.

Title Page

Abstract	Introduction
Conclusions	References
Tables	Figures

◀ ▶|

◀ ▶

| Back | Close |

Full Screen / Esc

Printer-friendly Version

Interactive Discussion

Table 1. Volume equivalent diameters, calculated hygroscopic growth factors, calculated critical supersaturation and ε_G and ε_{CCN} of particles with a mobility diameter of $d_m = 100\,\text{nm}$ and various shape factors $X = \{1.00,\ 1.05,\ 1.10\}$. The particles are assumed to consist of 30% Levoglucosan and 70% insoluble material by volume.

X	d_{ve} (nm)	G	ε_G	S_c (%)	ε_{CCN}
1	100	1.13	0.11	0.52	0.1
1.05	95.8	1.08	0.066	0.54	0.087
1.1	92.0	1.04	0.030	0.58	0.067

Table 2. Calculated critical supersaturations (S_c) and diameter growth factors (GF) of an idealized biomass burning particle consisting of 30% levoglucosan and 70% insoluble material at temperature $T = 293$ K. ε_{CCN} denotes the effective soluble volume fraction derived from S_c and ε_G the effective soluble volume fraction derived from GF as described in sections 3.1 and 3.2 using ammonium sulfate as a model salt.

d_p	S_c (%)	GF	ε_{CCN} $(NH_4)_2SO_4$	ε_G $(NH_4)_2SO_4$	ε_{CCN} lev.	ε_{CCN} lev.
50	1.43	1.12	0.10	0.12	0.3	0.3
100	0.52	1.13	0.09	0.12	0.3	0.3
150	0.28	1.13	0.09	0.11	0.3	0.3

Water uptake of biomass burning aerosol

U. Dusek et al.

Title Page

Abstract | Introduction

Conclusions | References

Tables | Figures

◄ | ►|

◄ | ►

Back | Close

Full Screen / Esc

Printer-friendly Version

Interactive Discussion

Table 3. Calculated critical supersaturations S_c and effective soluble volume fractions ε_{CCN} for an idealized biomass burning particle consisting of 30% levoglucosan and 70% insoluble material at temperature $T = 293$ K, assuming that the surface tension at the point of activation is 0.9 and 0.8 time that of water. Calculations of ε_{CCN} are carried out for both ammonium sulfate and levoglucosan as a model substance. ε_{CCN} for the original particle (surface tension of water) are 0.10 for ammonium sulfate and 0.30 for levoglucosan.

d_p	S_c (%) 0.9σ	S_c (%) 0.8σ	ε_{CCN} 0.9σ $(NH_4)_2SO_4$	ε_{CCN} 0.8σ $(NH_4)_2SO_4$	ε_{CCN} 0.9σ lev.	ε_{CCN} 0.8σ lev.
50	1.22	1.03	0.14	0.2	0.42	0.61
100	0.44	0.37	0.14	0.2	0.42	0.61
150	0.24	0.20	0.14	0.2	0.42	0.61

Table 4. Critical supersaturations and hygroscopic diameter growth factors (at 90% RH) for a particle consisting of levoglucosan and succinic acid in varying proportions. Calculations were made at temperature $T = 297$ K.

d_p (nm)	0% succ.		50% succ		90% succ	
	S_c (%)	GF	S_c (%)	GF	S_c (%)	GF
50	0.82	1.22	0.75	1.12	0.75	1.04
100	0.29	1.24	0.27	1.14	0.25	1.06
150	0.15	1.24	0.15	1.14	0.14	1.06

Water uptake of biomass burning aerosol

U. Dusek et al.

Table 5. Soluble volume fractions derived from CCN properties (ε_{CCN}) and hygroscopic growth factors (ε_G) for a particle consisting of levoglucosan and succinic acid in varying proportions. The respective values of S_c and GF used in the calculations can be found in Table 4.

d_p (nm)	0% succinic		50% succinic		90% succinic	
	ε_{CCN}	ε_G	ε_{CCN}	ε_G	ε_{CCN}	ε_G
50	0.31	0.32	0.32	0.16	0.36	0.07
100	0.29	0.33	0.34	0.18	0.39	0.07
150	0.31	0.32	0.37	0.16	0.40	0.05

Table 6. Soluble volume fractions (ε) and hygroscopicity parameters (κ) for freshly emitted wood burning particles. The values represent averages over all nine biomass burning experiments.

d_p (nm)	ε_G	ε_{CCN}	κ_G	κ_{CCN}
50	0.06	0.17	0.04	0.10
100	0.11	0.13	0.07	0.08
150	0.10	0.09	0.06	0.06

Table 7. Critical supersaturation (S_c), surface tension at activation (σ) and effective soluble volume fraction (ε_{CCN}) for a particle consisting of 30% levoglucosan, 5% fulvic acid and 65% insoluble material at various particle diameters (d_p).

d_p (nm)	S_c (%)	σ (mN m^{-1})	ε_{CCN}
50	1.09	63.3	0.18
100	0.45	66.8	0.13
150	0.26	69.1	0.11
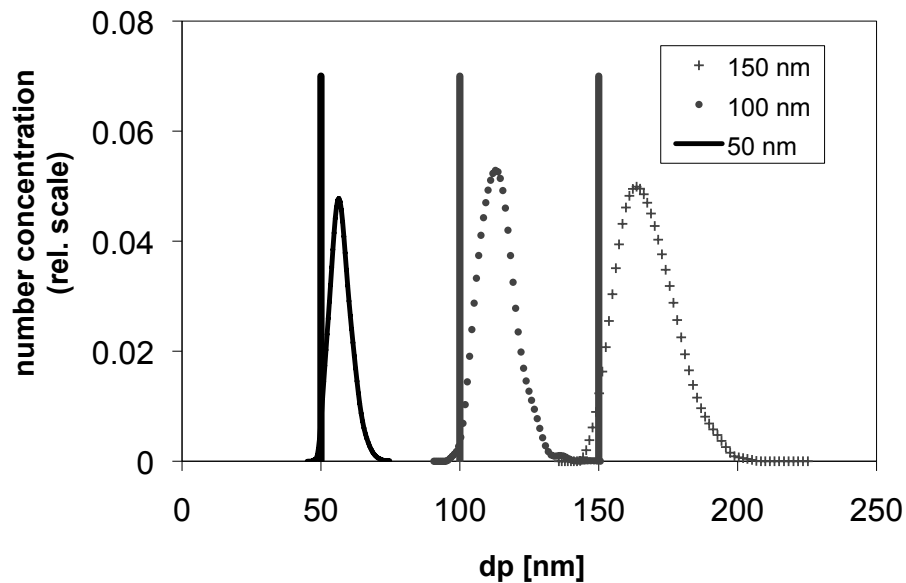
Fig. 1. Typical humidified size distributions as measured by the H-TDMA for particles with nominal dry diameters of $d_p = 50$ nm, 100 nm, and 150 nm (vertical lines).

Title Page

Abstract | Introduction

Conclusions | References

Tables | Figures

|◄ | ►|

◄ | ►

Back | Close

Full Screen / Esc

Printer-friendly Version

Interactive Discussion
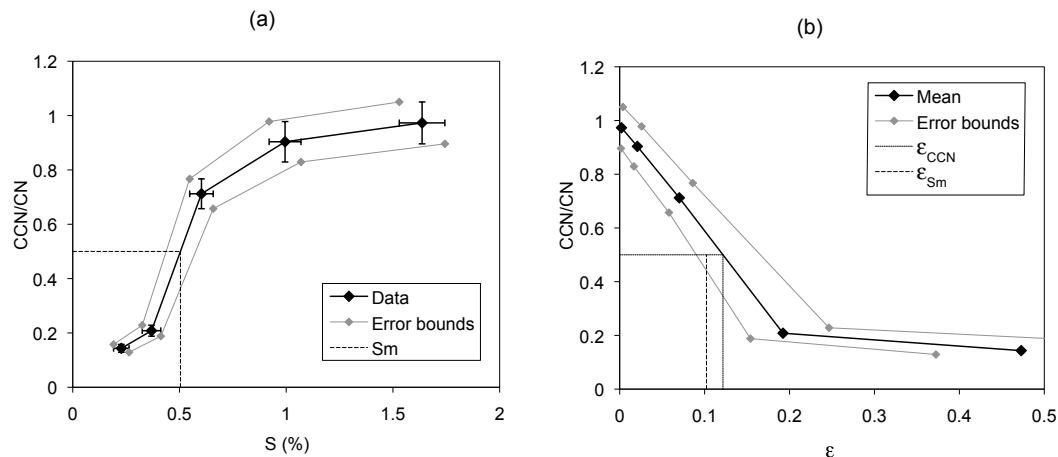
Fig. 2. The derivation of ε_{CCN} using 100 nm oak wood smoke particles as an example. **(a)** Average CCN spectrum of Experiment 14a (oak wood) including error bars indicating a measurement uncertainty of $\pm 1\sigma$ are shown as a black line and black symbols, upper and lower bounds of the activation curve (see Sect. 2.4) are shown as grey lines, and the supersaturation, where 50% of the particles are activated is indicated by a vertical dashed line. **(b)** The same CCN/CN ratios plotted as a function of ε corresponding to each S measurement point (black symbols and line) with error bounds (grey symbols and lines). ε_{CCN}, defined as the value of ε, where 50% of the particles are activated is indicated by a dotted line, and is substantially larger than the soluble volume fraction corresponding to S_c^m (ε_{Sm}; dashed line).
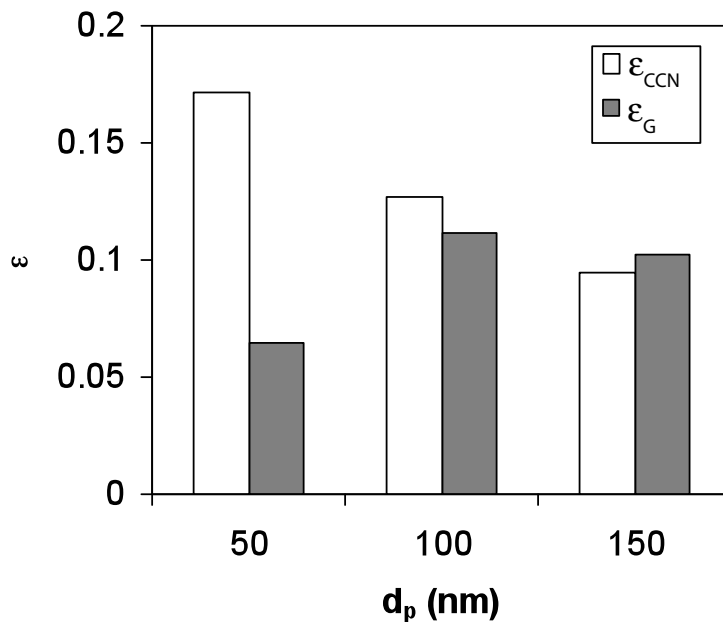
Fig. 3. Grand averages (of all nine experiments) of soluble volume fractions derived from hygroscopic growth factors (ε_G) and from CCN spectra (ε_{CCN}), using ammonium sulfate as a model salt.

Title Page

Abstract | Introduction

Conclusions | References

Tables | Figures

◄◄ | ►►

◄ | ►

Back | Close

Full Screen / Esc

Printer-friendly Version

Interactive Discussion

(a) 50nm
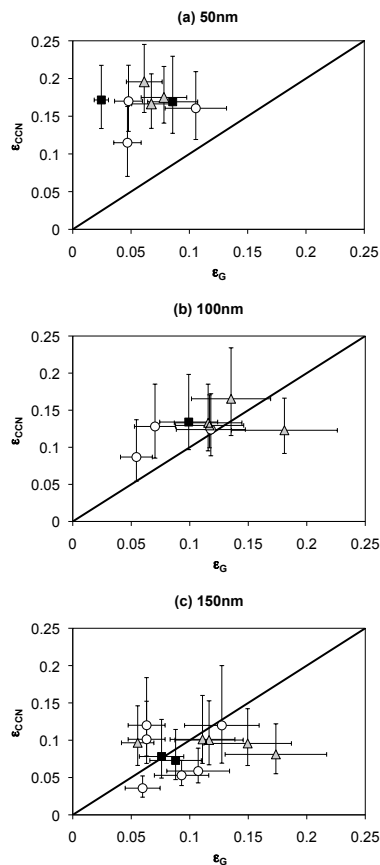
(b) 100nm

(c) 150nm

Fig. 4. Correlation between ε_{CCN} and ε_G at different particle diameters. Each data point represents an individual biomass burning event of approximately 1 h. Hardwood fuels (musasa, oak) are indicated as black squares, softwood fuels (spruce, pine) as white circles, and softwood fuels including needles and branches as grey triangles.

Title Page

Abstract | Introduction

Conclusions | References

Tables | Figures

|◄ | ►|

◄ | ►

Back | Close

Full Screen / Esc

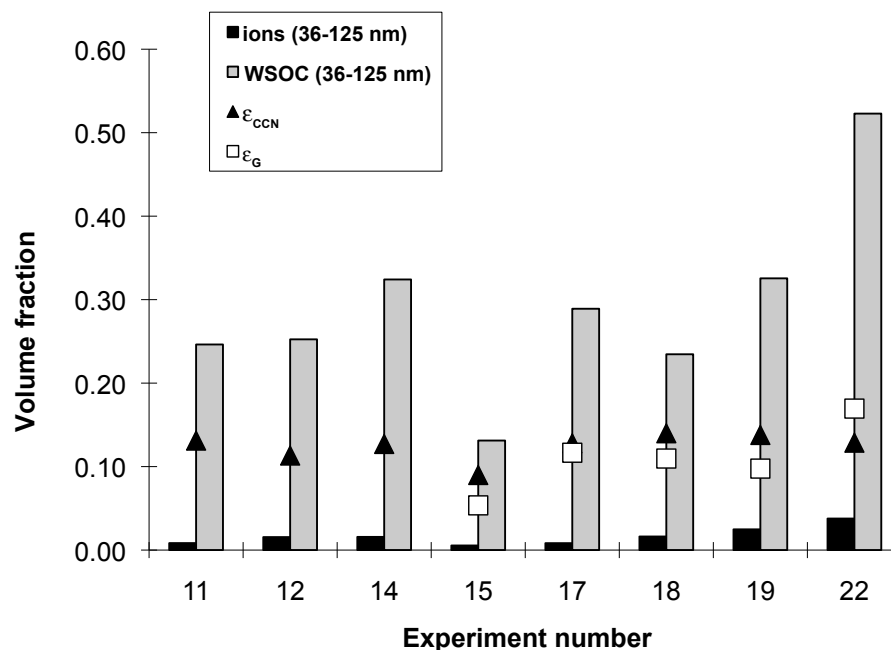Printer-friendly Version

Interactive Discussion

Fig. 5. A comparison of the volume fraction of inorganic ions (black bars) and water soluble organic carbon (WSOC; grey bars) estimated from impactor samples, with the effective soluble volume fractions derived from CCN measurements (ε_{CCN}) and hygroscopic growth factors (ε_G).

Discussion Paper | Discussion Paper | Discussion Paper | Discussion Paper |

ACPD

10, 29853–29895, 2010

Water uptake of biomass burning aerosol

U. Dusek et al.

Title Page

Abstract	Introduction
Conclusions	References
Tables	Figures

|◄   ►|

◄   ►

Back   Close

Full Screen / Esc

Printer-friendly Version

Interactive Discussion